Catalysis Science & Technology

Accepted Manuscript

ROYAL SOCIETY OF CHEMISTRY

www.rsc.org/catalysis

Journal Name

RSCPublishing

ARTICLE

New challenges for gold catalysis: bimetallic systems

Cite this: DOI: 10.1039/xoxxoooooox

Alberto Villa,[a] Di Wang,[b] Dang Sheng Su[c,d] and Laura Prati*[a]

Received ooth January 2012,
Accepted ooth January 2012

DOI: 10.1039/xoxxoooooox

www.rsc.org/

Since the discovery of the peculiar catalytic activity of gold catalysts, it clearly appeared that gold could have played a fundamental role also as a modifier. Indeed more active catalysts such as Pd or Pt based, acquired specific and sometimes unravelled properties when modified with gold. This paper reviewed advances in the field of Au based bimetallic catalysts with particular attention to their preparation, characterization and catalytic activity. AuPd catalysts, the most widely studied, have been chose as example to show how the different morphologies obtained (alloy, core-shell, decorated particles) can contribute to the catalytic activity.

Introduction

Metal nanoparticles have received a lot of interest in the last decade because of their unique properties finding potential applications in different fields, such us catalysis, electronics, optics, imaging, and biology.[1]

In particular, Gold have been now reached an established important role in the field of catalysis since, twenty years ago, Haruta and Hutchings disclosed the peculiarity of the activity of this metal in CO oxidation and ethylene hydrochlorination.[2,3] The use of gold in catalysis has been enormously expanded but,[4] since the beginning of its story, the use of gold for manufacturing new catalytic systems was affected by the high variation of the catalytic performances depending on the preparation method employed and the support used.[5] Indeed, many studies stated the importance of preparation and support in determining the morphology of the gold particles and metal-support interaction, both able to profoundly modified the activity and/or the selectivity of the whole catalyst. Therefore a lot of attention had been paid to the preparation of gold catalysts for assessing as much as possible the relation between support/preparation method and characteristics of the produced materials

Gold has shown particularly attractive behavior in both selectivity and resistance to deactivation compared to Pd and Pt catalysts.[6] The durability of the catalysts currently restricts the industrial application of metal supported catalysts, in particular, in liquid phase oxidations when dioxygen or air are used as the oxidant.[6] On the other hand, a serious drawback for industrial exploitation of gold catalysts was the apparent need of the presence of a base.[7]

Bimetallic systems can overpass the latter limitation, combining the properties associated with the two constituent metals.[8] In most cases, there is a great enhancement in their specific physical and chemical properties owing to a synergistic effect. The kinetic of the reaction, the selectivity to the desired product and the durability of the catalyst have been shown to be speed up by the alternative use of bimetallic species where gold improved the performances of other metals like Pd, Pt and Ru.[9]

The superior performance of bimetallic systems compared to monometallic counterparts has been reported for different chemical reactions, including CO oxidation[10] the selective oxidation of alcohols to aldehydes,[9,11] the direct synthesis of hydrogen peroxide,[12] the oxidation of primary C-H bonds,[13] the transformation of biomass to fuel and chemical.[14]

However, the nature of the synergistic effect often observed from an experimental point of view, is not always completely understood from a surface science point of view even much efforts have been put on this task.[15] The reason of this lack lies on the variety of possible combination of reactant, composition, and experimental conditions. Moreover a lot of experimental data have been obtained with catalytic systems that have not wholly characterized letting some doubt on their real morphology (alloy, core-shell, decoration) and homogeneity. This in turn has greatly limited the determination of a direct correspondence between the structure of bimetallic systems and their catalytic properties, most of the times providing single example of application.

The aim of this review is to provide a critical contribution highlighting the advances in this field through the most significant

examples in the use of gold based bimetallics. Among them AuPd catalyst is the most extensively studied. In general, bimetallic system, according to their mixing pattern, could have the following four structural types : i) core-shell segregated nanoparticles with a shel of type A atoms covering a core of type B atoms (Figure 1a): subcluster segregated nanoparticles consisting of A and B subcluster that share a mixed interface (Figure 1b): iii) mixed nanolaaloys of two type atoms being either ordered or solid solution (Figure 1c): iv) multishelled nanoparticles with layered or onion-like alternating shells (Figure 1d).[16]

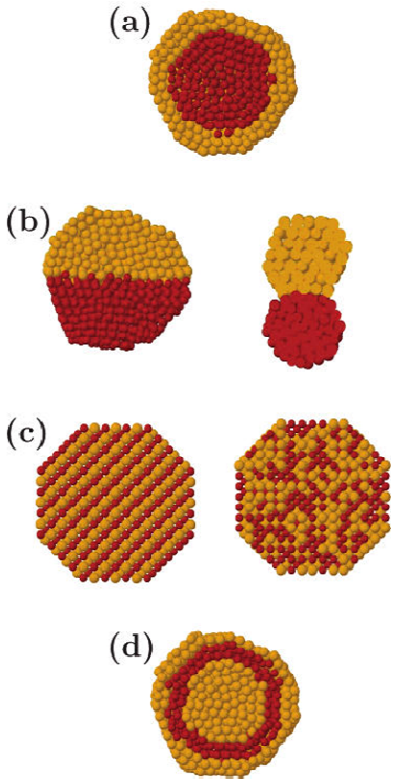

Figure 1. Schematic representation of some possible mixing patterns: core-shell (a), subcluster segregated (b), mixed (c), three shell (d). The pictures show cross sections of the clusters. Reprinted (adapted) with permission from Ref 16. Copyright (2008) American Chemical Society

Au is miscible with Pd in all the compositions, and therefore this facilitates obtaining AuPd alloys limiting segregation of single metals. Moreover, AuPd showed promising results in different catalytic application, such as alcohol and polyols oxidation , direct production of H_2O_2 from H_2 and O_2, C-C coupling and CO oxidation.[9-14] In this review, we will focus our attention on the application of Au-Pd systems in the selective liquid phase benzyl alcohol oxidation and the gas phase CO oxidation trying to highlight the correlation between the structure and the performance of the catalyst. The first reaction plays an important role from a synthetic point of view and, when carried out as a catalytic process with O_2 as the oxidant, provide a green and sustainable alternative to the use of stoichiometric oxidant.[9] On the other hand CO oxidation is of great importance in fundamental research as well as in application of industrial interest such us air clean-up,[17] automotive pollution control[18] and in the removal of CO traces in H_2 in fuel cells.[19] A brief survey on the available preparation methods and the characterization techniques of Au-Pd bimetallic systems will be provided before discussing the relationship between the structure and the catalytic performances

Synthesis of AuPd systems

Different synthetic strategies have been proposed for the preparation of bimetallic systems. In this section we will summarize the most used for the preparation of gold bimetallic catalysts dedicated to the liquid and gas phase oxidations. Among them, metal sol immobilization and the direct impregnation of metal salts are the most reported.

The first method is based on the preparation of bimetallic by co-reduction or consecutive reduction of metal precursors in the presence of a stabilizing agent which acts to passivate the nanoparticles surface and prevent them from aggregation, and their subsequent immobilization on a support.[20] In the catalyst preparation by immobilization of metal colloid, it is very important to be able to separate the nucleation and the growth into different steps, as suggested by Lamer et al.[21] The reducing agent and the protective agent play a fundamental role on the structure of the final catalyst, being both important for example to tune the size of the metal nanoparticles. Normally the use of a strong reducing agent, such as $NaBH_4$, is needed in order to simultaneously reduce both metals, but a quick metal reduction makes the nucleation and growth processes difficult to control. In such a case the use of an appropriate protective agent can passivate the surface of the cluster making the process easier to be controlled. Employing this strategy it is possible, in theory, to tune the morphology of the bimetallic system. When the second metal with lower redox potential is reduced, it can deposit on the surface of the preformed nucleus of the first metal symmetrically with a core/shell structure. If the two metals are completely miscible, as in the case of Au Pd, an alloy can be formed.

The stabilization against agglomeration can be achieved by electrostatic, steric or electrosteric effect.

Electrostatic stabilization is based on the mutual repulsion of electrical charges. When two similar particles, are close to each other, the van der Waals force resulting from electromagnetic effect is always attractive. The addition of a protective agent, such as citrate or tetrakis-(hydroxymethyl) phosphonium chloride (THPC), on the metal precursor (i.e.metal halides) generated an electrical double layer of cations and anions. The adsorbed layers results in Coulombic repulsion between the particles resulting in stabilization of the colloid. For example, Baiker and co-workers reported the synthesis AuPd catalyst by coredcution of Au and Pd halides in presence of Tetrahydroxymethylphosphoniumchloride (THPC).[22] THPC is an electrostatic stabilizer, the negatively charged Au and Pd precursors coordinate with the positive part of the THPC molecule. During the formation of the metallic sol, a huge excess of NaOH is present. THPC/NaOH, acts as the reducing

agent by the formation of formaldehyde, a well-known reducing agent for gold under basic conditions following the mechanism:

$P(CH_2OH)^{4+} + OH^- \rightarrow P(CH_2OH)_3 + CH_2O + H_2O$.[23]

Sodium Citrate, as well, has been widely used as electrostatic protective agent in particular for monometallic Au. Sodium citrate acts as stabilizer as well as deucing agent. In particular during the metal reduction it becomes oxidized to the intermediate ketone (acetone dicarboxylic acid), which in turn is an even better reducing agent. Guczi's and co-workers used this methodology for the synthesis of AuPd bimetallic system supported on TiO_2. AuPd nanoparticles were generated in presence of tannin and citrate, in aqueous solution at 338K and immobilized on TiO_2.[24] The steric effect has been obtained by absorption of e polymers of sufficiently high molecular weight, forming a protective layer and keeping the nanoparticles at a distance too large to give a van der Waals interaction, therefore avoiding agglomeration. Among them, polyvinyl pyrrolidone (PVP) is the most used.

Venezia et al. prepared AuPd catalysts on silica using PVP as protective agent.[25] Au and Pd halides precursors have been simultaneously added to a water/ethanol solution containing PVP (metal/PVP ration 1/5 wt/wt). Silica has been added and left under stirring at 363K for 5h under N_2 till complete reduction.

Electrosteric stabilization has been achieved by the adsorption polymers having non-negligible electrostatic charge on the metal precursors, resulting in a significant double-layer repulsion. Polyvinyl alcohol (PVA), is atypical example and it is by far the most employed stabilizer used for the generation of AuPd nanoparticles.[26] The effect of the sequence of Au and Pd precursors addition has been investigate. Au and Pd have been reduced in presence of PVA simultaneously or by sequential reduction usually using $NaBH_4$ as reducing agent.

The simultaneous reduction of Au salts in a proper solvent in the presence of a protective agent followed by their immobilization on a support has been widely reported.[27] The fundamental step for obtaining bimetallic nanoparticles is the control of the reduction and the nucleation processes of the two metals, because of their different redox potential and the different chemical nature. Therefore, In order to avoid any segregation of the two metals a proper reducing agent and/or proper reaction system should be selected.

Prati e al was among the firsts to prepare PVA protected AuPd nanoparticles for liquid phase reaction. Firstly, they reported the formation of an alloy when carbon supported Au-Pd (Au:Pd= 1:1 molar ratio) bimetallic catalyst has been prepared using polyvinyl alcohol (PVA) as protective agent and $NaBH_4$ as reducing agent, even partial segregated Palladium was detected.[27b] On the contrary Hucthings' group using the same methodology for preparing Au-Pd catalysts supported on activated carbon and titania, obtained pure alloy.[27h] This difference could be addressed to the different amount of polyvynilalcohol (PVA) used: PVA/metal 2:1 in the first case and PVA/metal 1:2 in the second. A higher amount of protective agent probably limits the diffusion of Pd in the gold nanoparticles and segregation of Pd is observed.

The second approach utilizes a preformed nanoparticles of the first metal and subsequently directing the deposition of the second metal onto a surface site with a specific geometry. This method is commonly used to prepare core–shell.[28] When the second metal deposits on the surface of preformed seeds, a core-shell structure can be obtained, whereas alloy or heterostructures can be synthesized when the deposition and growth of the second metal occurs on a specific site.[27b,29] Moreover the kinetic of the growth of the second metal on the preformed seed can tune the final structure. Different structures have been obtained, for example, for Au-Pd catalyst, according to the protective and reducing agent used. The reduction of palladium followed by the one of gold leads to a mixture of the two metals in the colloid solution due to the weakness of the reducing agent and only after aging, an alloy has been obtained. On the contrary when Au has been deposited on Pd, bimetallic particles are immediately formed without detection of Pd_{core}-Au_{shell}. Probably during the addition of Au, Pd(0) atoms on the nanoparticles are oxidized to Pd^+ with the reduction of Au(III) to Au(0). After the addition of the reducing agent Pd ions formed are then reduced again with the formation of a complex structure.

Our group reported the synthesis of Au-Pd catalyst by successive reduction of Au in presence of Pd metal sol and Pd on Au sol before immobilization on carbon.[27b] The reduction has been performed by $NaBH_4$ for both metals in presence of PVA as a protective agent. The bimetallic nanoparticles obtained, with an average diameter of 3.5 nm, showed an alloy structure with the presence of segregated Pd. A second strategy consists, in the immobilisation of a preformed gold sol using $NaBH_4$ as reducing agent on activated carbon, and then the sol of palladium was generated in the presence of Au/C using H_2 as a second reducing agent instead of $NaBH_4$.[29] Using H_2 instead NaBH4 it was possible to slow down the reduction rate of the Pd ions thus increasing the time of the diffusion and growth of Pd on Au avoiding any Pd segregation (Figure 2).

The Au-Pd alloy nanoparticles showed uniform composition and homogeneity. In further studies Au-Pd with different ratio (Au:Pd; 9.5:0.5, 9:1,8:2,6:4,2:8) has been prepared using the same procedure to investigate the effect of different Au/Pd ratio on the final structure of the bimetallic alloy.[30]

Moreover, the role of the protective agent of the Au precursor, on the formation of an alloy of uniform composition has been investigated.[31] For this purpose three different gold precursor has been prepared using, a steric stabilizer (PVA), and electrostatic stabilizer (THPC) or without any protective agent (Au prepared by magnetron sputtering). Only when AuPVA system has been used, Au-Pd uniform alloy has been obtained.

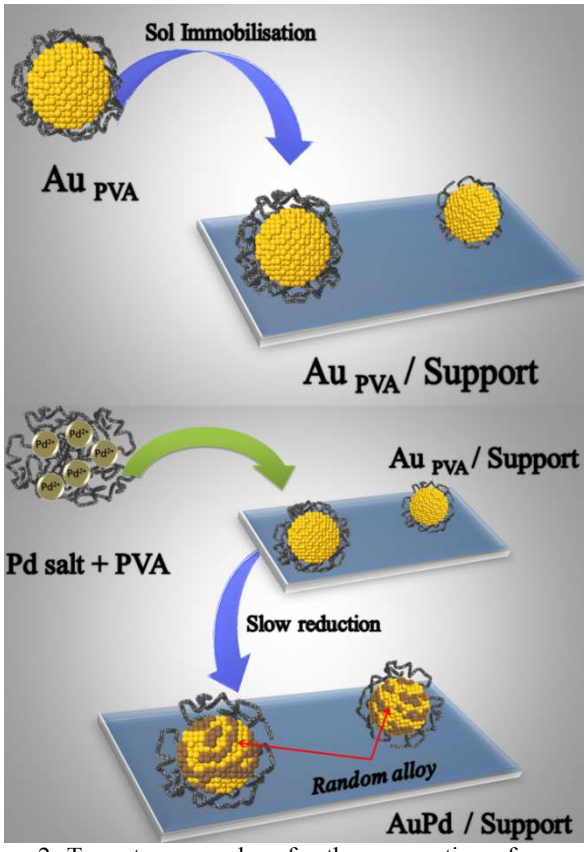

Figure 2. Two-step procedure for the preparation of supported AuPd uniform alloy

Unprotected Au or weakly stabilized Au (THPC) NPs undergo reconstruction during the deposition/reduction of Pd, not providing efficient seeds for alloying the Pd. In these latter cases, growing of Au, segregation of the two metal or formation of different alloy composition has been observed.

Recently Tiruvalam et al. showed the formation of PdcoreAushell and $Au_{shell}Pd_{core}$ by successive reduction, using a similar methodology used in Ref. 27b.[28] However, as it will be stated in the following section, it is always difficult to prove the presence of a real core-shell structure or Pd-rich or Au-rich bimetallic catalysts, in presence of particle size below 10nm.

The impregnation method consists in the direct impregnation of an aqueous solution containing the metal precursors the support in absence of any protective agent followed by evaporation of the water. The dried material is further subject to reduction normally by high temperature treatment or gas phase reduction under flow of H_2.[32] The characteristics of the catalyst strictly depend on the post-treatment conditions (rate of heating, time, final temperature, atmosphere) and, obviously, on the type of supporting materials. In fact during the calcination step sintering of the precursor and reaction between the metal precursor and the support might occur. Moreover the use of different conditions can lead to different metal-support interaction, of fundamental importance for the catalytic applications. As the effect of temperature is normally detrimental from the metal dispersion point of view, sometimes a reduction step with H_2 or, under basic conditions, with HCHO or $NaBH_4$ have been used instead of calcination.[32] Even impregnation has been shown to produce less active gold catalysts than sol immobilization, the simplicity of the methodology make impregnation still attractive for industrial scale-up purposes, and because of that, much research has been dedicated to improve the preparation method.[32]

This technique has widely been used for the preparation of Au-Pd on titania and carbon in particular by Hutchings' group.[33] In a typical preparation $AuCl_4^-$ is dissolved in water and then $PdCl_2$ is dissolved in the resulting acidic solution. The support is then contacted with the solution and then dried (383K, 16 h) and calcined (673K, 3 h). Heat treatments steps are very important and control the final morphology obtained. The support plays a fundamental role on the final structure of AuPd. Indeed, on carbon supports random AuPd alloys are formed, whereas for oxidic supports, such as TiO_2 core-shell structures are formed with a gold-rich core and a palladium-rich shell.[11b] The heat treatment steps normally leads to a grown of particles size, being more evident of carbonaceous support compared to metal oxides.

Summarizing this part, the advantage of using sol immobilization principally lies in the applicability regardless the type of support employed and the possible control on particle size/ distribution, obtaining normally highly dispersed metal catalyst. On the contrary direct impregnation is drastically affected by the surface properties of the support. To be noted that in the preparation of bimetallic catalysts particular attention has to be paid to the composition of the single metallic particles in terms of ratio of metals and morphology.

Characterization of AuPd

Alloying with gold by a second metal or even by more metals has increased largely the possibilities to tailor the structures therefore the reactivity of the catalysts. The structure complexity increases at the same time. In addition to particle size and shape, the composition, distribution and surface ordering should be taken into consideration for affecting the activity, selectivity and stability of the catalysts. In order to correlate specific sites on the bimetallic systems to catalytic properties, the catalysts structures need to be characterized at nanometric up to even atomic scale. Complementary X-ray spectroscopic and electron microscopic characterization methods can be used to derive the structural information about the atomic configuration on particle surfaces, inside particles and at the interfaces.

X-ray techniques derive mainly average structures from the catalysts. X-ray diffraction (XRD) is widely used to determine the phase consisted in the catalyst, mainly crystalline support and the metallic particles. When metal components with different lattice parameters are segregated, XRD usually can distinguish two different phases. When random alloy is formed, it can often be detected by precise determination of the changed lattice parameter, which is different from either monometallic counterpart. In addition, according to Vegard's Law[34] and Rietveld analysis[35] ratio of the two alloying metals can be

estimated. XRD is also widely used to evaluate the particle size from the width of the diffraction peak.[36] However it is not sensitive to particles as small as 1-2 nanometers. Therefore (S)TEM imaging are more preferred for quantitative measurement of the particle size in catalyst. Based on HAADF STEM, several analytic methods have been developed to precisely measure the particles size, e.g., by integrating the intensity from the area of cluster to quantify the number of atoms in it, or by blurring propagation method.[37,38]

X-ray photoelectron spectroscopy (XPS) is a surface sensitive technique, which provides not only the composition on particle surfaces but also valence states according to the binding energy of inner shell electrons.[39] It is of particular interests for bimetallic particles synthesized following different procedures to tailor the distribution of two metals from core-shell structure to random alloys. Some calcined supported Au-Pd catalysts have been characterized by XPS and showed Pd-enriched surface and Au was suggested to promote the Pd by electronic effect.[11b,40] Pd^{2+} has been detected by XPS on monometallic Pd catalysts, while by adding small amount of Au to form Au:Pd = 1:9 bimetallic particles it is already enough to keep all the Pd atoms as Pd(0). In many literatures, it has been reported that Au 4f7/2 peak shifts to lower energy by alloying with Pd and this shifts deceases further with decreasing the Au concentration.[22,41–43] This could be due to increased Au 5d occupancy. It was suggested that negatively charged Au could facilitate the extraction of beta hydrogen of the alkoxide intermediates.[11] One should also be aware that the material within the depth of a few nanometers may contribute to the photoelectron signals. Therefore for nanoparticles, results are more weighted for the top surface atomic layers but particle core contributes also attenuated signals.

With X-ray absorption spectroscopy (XAS),[44] the near edge structure of ionization edges of Au and other metals can be recorded to study the electronic states modification due to alloying as well as due to metal-support interaction. Furthermore analysis of extended X-ray absorption fine structure (EXAFS) is unique to provide the structural information of coordination number of a certain type of inter atomic bonding and the distances between atoms. Though XAS is not location specific technique, in combination with TEM and spatially resolved spectroscopy, which reveal the particle size distribution and the compositions in nanoparticles, it can provide valuable information about the atomic configuration of bimetallic nanoparticles. Au-Pd bimetallic catalysts following the redox procedure, colloidal method and other synthetic methods were characterized by X-ray absorption near edge structure (XANES) and EXAFS.[22,41,42,45] For Au deposited onto activated carbon supported Pd, XANES of Pd K edge and Au L edge confirmed that Au-Pd is in metallic state in contrast to oxidative Pd for monometallic catalyst. EXAFS has shown that the first shell Pd-Pd coordination number doesn't change much for bimetallic catalysts compared to the monometallic one. There was small amount of Pd-Au coordination arising from Au-Pd interactions. These results indicate that Pd particles were relatively unaltered by depositing Au on it and Au was dispersed on Pd surface. In contrast, EXAFS characterization of AuPd(sol) catalysts shows more highly dispersed Pd.[45] Therefore the distribution of Au and Pd is highly dependent on the catalyst preparation method. The coordination numbers of Au-Au, Au-Pd and Pd-Pd are systematically studied for bimetallic catalysts with different Au:Pd ratios[22,41] and different core-shell structures were formed depending on the synthesis method and Au:Pd ratio. The intensity of XANES edges often reflects the occupancy of empty orbitals, into which the atomic electrons are excited. For example it has been reported that Au L_{III} white lines intensity decreased with decreasing particle size, as well as with decreasing Au concentration for Au-Pd bimetallic catalyst, which was attributed to more electron occupancy in Au 5d. The results clearly indicate that highly dispersed Au clusters caused change in electronic property.[22,41,42]

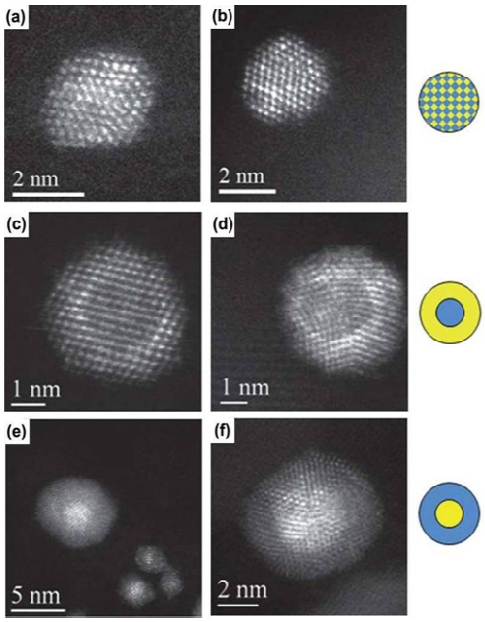

Figure 3. Representative HAADF-STEM images of individual sol-immobilized (Au + Pd) (a), Au{Pd} (c), Pd{Au} (e) NPs on activated carbon, and (Au + Pd) (b), Au{Pd} (d), Pd{Au} (f) NPs on TiO_2 after drying at 120 °C for 16 h. Reproduced from Ref. 28 with permission from The Royal Society of Chemistry

Complementary to the X-ray characterization techniques, TEM provides direct imaging of the catalysts up to atomic resolution and the distribution of elements can be resolved within individual nanoparticles. High-resolution transmission electron microscopy (HRTEM) and high angle annular dark field (HAADF) STEM images can reveal the atomic configurations of small particles with state of the art spherical aberration corrector[46] for objective lens and/or probe forming lens. Therefore the morphology, crystal structure, surface modification and capping, straining due to twinning or metal-support interaction can be unraveled. Particularly, HAADF STEM, due to its contrast mainly coming from incoherent thermal scattered electrons at high angle, the intensity can be directly correlated to the atomic number and sample thickness

along beam direction forming so called "Z-contrast" image.[47] It offers an intuitive interpretation for the HAADF STEM image from supported metal catalysts, where the support usually consists of light atoms, like in the cases of C support and metal oxide support. High resolution HAADF STEM image even resolves the position of different metal atoms on a single particle. The powerful application to use HAADF STEM studying some AuPd bimetallic structure showing in Figure 1 is displayed in Figure 3. More practically, energy dispersive X-ray spectroscopy can be acquired in STEM mode with a focused electron beam in size of sub nanometer. Recently, combining probe corrected STEM and in column silicon drift detector has improved the resolution and detector efficiency greatly so that core-shell structures, segregations and random alloys within individual particles can be unambiguously distinguished.

Efforts has been dedicated to synthesize different types of bimetallic nanoparticles and to characterize them with advanced TEM techniques.[48–53] It has been unraveled that the structure of bimetallic catalysts is dependent on support materials, the synthesis procedures and the post treatment to the as prepared catalysts. The inhomogeneity in composition and distribution is usually related to the ratio of alloyed metals and the specific particle size. For example, for the catalysts prepared by co-impregnation of the supports using incipient wetness with aqueous solutions of $PdCl_2$ and $HAuCl_4$ and following calcination at 400 °C, the Au-Pd particles on TiO_2 and Al_2O_3 as supports were found to exhibit a core-shell structure, Pd being concentrated on the surface. In contrast, the Au-Pd/carbon catalyst exhibited Au-Pd nanoparticles which were homogeneous alloys. The structure of bimetallic catalysts synthesized by sol immobilization method can be controlled by the sequence of reduction of metal precursors, namely $PdCl_2$ and $HAuCl_4$. Random alloy, Au core–Pd shell and Pd core–Au shell structure can be formed by reduction of mixed precursor solution, reduction of $PdCl_2$ in existence of Au(0) and reduction of $HAuCl_4$ in existence of Pd(0), respectively.[28] A STEM-EDX spectrum image analysis is presented in Figure 4, where both reconstructed RGB maps of Au and Pd, and integrated EDX spectra from the center and periphery of the particle confirmed a Pd core–Au shell structure. Similar successive reduction method has been used to produce three-layer core-shell particles, which consist of an alloyed inner core, an Au-rich intermediate layer, and a Pd-rich outer shell as revealed by HAADF STEM and EDX analysis.[54] The order of metal addition and reduction during initial sol formation affects not only the activity, but also the selectivity. A series of catalysts with Au:Pd ratios varying from 9.5:0.5 to 2:8 were synthesized following a two-step procedure.

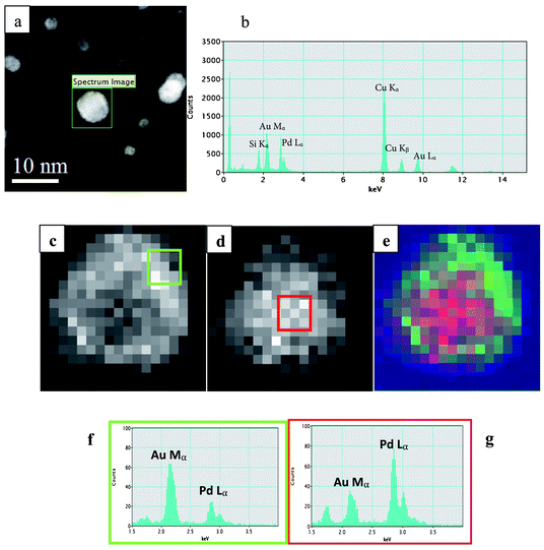

Figure 4 (a) An ADF image of an Au{Pd} nanoparticle selected for STEM-XEDS mapping; (b) The overall XEDS spectrum from the nanoparticle showing the presence of both Au and Pd; (c, d). The Au and Pd elemental maps of the nanoparticle obtained after MSA processing: (e) An RGB reconstruction showing the distribution of Au (green) and Pd (red)-the blue channel is neutral; (f, g) the cumulative XEDS spectra from 3 × 3 pixels (indicated by squares in (c & d)) from the center and periphery of the particle respectively. Reproduced from Ref. 28 with permission from The Royal Society of Chemistry

By HRTEM and STEM-EDX mapping it has been suggested that good alloy particle can be formed for the Au:Pd ratio of 9:1, 8:2, and 6:4, while the catalyst with Au:Pd = 9.5:0.5 and Au:Pd = 2:8 consist segregated Pd particles and were considered as the reason of low activity and quick deactivation in oxidation of glycerol.[30b]

In the liquid phase oxidation of benzyl alcohol, it was found that the structures of catalyst particles change dynamically with the reaction proceeding.[55] Physically mixed Au/AC and Pd/AC was used as starting catalyst. In situ formation of of surface Au-Pd bimetallic sites by reprecipitation of Pd onto Au nanoparticles was verified by STEM-EDX mapping on the catalysts after 0.5h and 1h of reaction. Figure 5 shows the STEM image, Au and Pd maps and the superimposed two maps of a few alloy particles formed after one hour reaction. Pd concentration increased with time on the initial Au particles. Negligible Au leaching was observed. When bimetallic sites are formed Au stabilises Pd atoms, thereby preventing Pd aggregation and leaching, which leads to deactivation of the catalyst. Until now not much has been done on the dynamical structure change during liquid phase reaction, partially due to difficulty in applying in situ characterization techniques to liquid systems. Nonetheless, depending on the miscibility of the alloying metals, the detailed structure of bimetallic particle and the reaction condition, one would expect that the catalysts commonly undergo changes during reaction, leading to segregation or enhanced alloying, therefore influence greatly the ultimate activity, selectivity and stability of the catalyst.

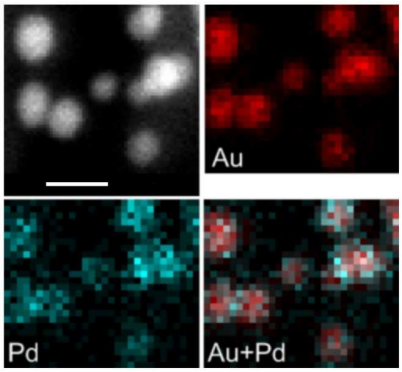

Figure 5 STEM images, Au and Pd maps and the superimposed two maps from one piece of original Au/AC in the physically mixed catalyst after 1 hour reaction of benzyl alcohol oxidation. Reproduced by permission from ref. 30b Copyright © 2010 WILEY-VCH.

As we can see form the above discussion, X-ray and TEM characterizations can provide complementary structural information for the determination of geometric and electronic structures of bimetallic nanoparticles. By different synthetic procedures, the structures of the nanocatalysts can be tailored to some extent therefore the activity and the selectivity can be controlled.

Catalytic applications

Benzyl alcohol oxidation

Benzyl alcohol has been extensively used as a model reaction in particular for aromatic activated alcohol.[6] Depending on the reaction conditions (temperature, solvent, oxygen pressure), many side-products including benzene, benzoic acid, benzyl benzoate, and toluene have been reported to be formed besides the main product benzaldehyde, as shown in Scheme 1.

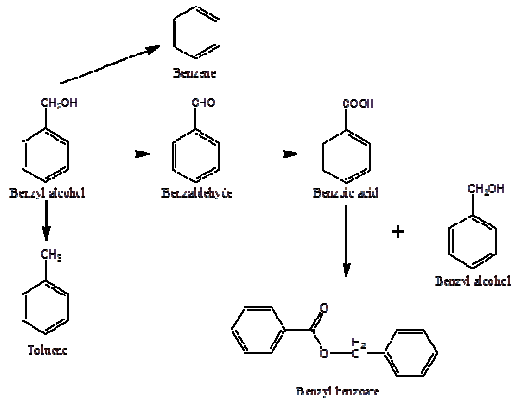

Scheme 1. Reaction scheme for benzyl alcohol oxidation

Many papers reporting the utilization of AuPd systems in the benzyl alcohol oxidation are present in the literature but an exhaustive comparison is not possible due to the different reaction conditions used. Typically, these reactions are performed in a batch reactor under mild conditions with temperatures in the range of 333-393 K and partial pressure of O_2 of 1-10 bar, in the presence of solvents, such as cyclohexane, toluene and water, or under solventless conditions.

Different preparation methods, in particular sol immobilization with PVA as protective agent and impregnation have been used. Moreover, a wide range of supports, such as activated carbon, carbon nanotubes, TiO_2, SiO_2 and polymers have been considered.[6,9] Some examples are reported in Table 1.

Prati's group were among the first to demonstrate the efficiency of using sol immobilization method for making AuPd uniform pure alloy supported on activated carbon and to test this catalyst for alcohol oxidation in the presence of O_2.[11a] It was demonstrated that the presence of AuPd alloy increases the catalytic activity compared to the monometallic Pd (TOF of 38 to 54 h^{-1}, for Pd and AuPd, respectively) (entry 1 and 2, Table 1), keeping a very high selectivity (>94%) to benzaldehyde. To note that under the same conditions Au was inactive. The better activity has been ascribed to a geometric effect. Indeed, in AuPd the interatomic distances, are different than in the pure metals.[29] A significant improvement in the catalytic activity was found when water was used as solvent instead of toluene, with a TOFs values that increased from 54 h^{-1} in toluene to 985 h^{-1} (entry 5, table 1). The beneficial effect of water could be ascribed to the modification of the affinity of the substrate for the hydrophobic catalyst surface of the activated carbon, favoring the adsorption of the alcohol and the desorption of the carbonyl compound. Moreover, the abstraction of the hydride, the rate-determining step in the oxidative dehydrogenation of alcohol is favored in the presence of water, a weak base.[6] Interestingly, under these reaction conditions, the presence of water as solvent did not show any effect on the selectivity, with benzaldehyde as the unique product. AuPd alloy did not only show a higher activity than Pd but also a better resistance to deactivation.[27g,56] The presence of Au indeed, drastically limits the deactivation typical of Pd, due to leaching of the metal and deactivation by O_2 poisoning.[11a] Using the same preparation method, it was demonstrated the general applicability of single phase alloy with Au/Pd molar ratio varied from 9-1 to 2-8 (entry 3-10, table 1). The best performance have obtained when uniform alloyed bimetallic nanoparticles were obtained (Au/Pd range 9:1-6/4, entry 3-5, table 1), and in particular Au8-Pd2/AC was the most efficient (entry 4, table 1). On the contrary Au2-Pd8/AC, where Pd monomer sites isolated by Au atoms were present, showed a slight lower activity (entry 6, table 1). Moreover it has been showed that, as expected, the addition of a base increases the activity of the catalysts (entry 7-10, table 1). It is well recognize that the presence of base favors the abstraction of the hydride, the limiting step for Au catalyzed alcohol oxidation.[6] Interestingly, this effect is more evident for Au-rich composition. The authors stated that in gold rich-composition the rate determining step is the H-abstraction, whereas in the Palladium rich composition is the H-transfer from Pd-H, where the base has a negligible effect.[57] The addition of a base resulted detrimental in terms of selectivity with the formation of benzoic acid and benzyl benzoate in high

Table 1 Comparative data for benzyl alcohol oxidation

Entry	Catalyst	Reaction conditions				TOF	Selectivity				Ref.
		Solvent	T (K)	pO_2 (bar)	Metal/ sub. ratio		Benzaldehyde	Toluene	Benzyl benzoate	Benzoic acid	
1	1%Pd/AC	toluene	333	1.5	1/500	38	>99	-	-		11a
2	1%Pd40@(Au60/AC)	toluene	333	1.5	1/500	54	94	-	-	-	11a
3	1%Pd10@(Au90/AC)	water	333	1.5	1/500	780	>99	-	-	-	57
4	1%Pd20@(Au80/AC)	water	333	1.5	1/500	1021	>99	-	-	-	57
5	1%Pd40@(Au60/AC)	water	333	1.5	1/500	985	>99	-	-	-	57
6	1%Pd80@(Au20/AC)	water	333	1.5	1/500	716	>99	-	-	-	57
7	1%Pd10@(Au90/AC)[a]	Water	333	1.5	1/500	1140	28	-	32	40	57
8	1%Pd20@(Au80/AC)[a]	water	333	1.5	1/500	1189	46	-	22	32	57
9	1%Pd40@(Au60/AC)[a]	water	333	1.5	1/500	1071	45	-	24	31	57
10	1%Pd80@(Au20/AC)[a]	water	333	1.5	1/500	776	50	-	24	26	57
11	5%Au50-Pd50/TiO_2	none	383	1	nd	14270	nd	nd	nd	nd	11b
12	5%Au50-Pd50/TiO_2	none	393	1	nd	26400	nd	nd	nd	nd	11b
13	5%Au50-Pd50/TiO_2	none	433	1	nd	86500	nd	nd	nd	nd	11b
14	1% Au+Pd/AC_{SI}	none	393	10	1/55000	1800	79	2	-	4	26f
15	1%Au+Pd/AC_I	none	393	10	1/55000	500	69	10	-	3	26f
16	1%Au+Pd/TiO_2	none	393	10	1/55000	15360	69	27	2	2	26g
17	1%Pd50@Au50/TiO_2	none	393	10	1/55000	19250	77	18	3	2	26g
18	1%Au50@Pd50/TiO_2	none	393	10	1/55000	17360	72	23	3	2	26g
19	1%Au50+Pd50/AC	none	393	10	1/55000	35400	55	41	2	1	26g
20	1%Pd50@Au50/AC	none	393	10	1/55000	41930	63	35	0	2	26g
21	1%Au50@Pd50/AC	none	393	10	1/55000	24310	65	29	3	3	26g
22	1%Au+Pd/TiO_2 calc. 673K	none	393	10	1/55000	3940	70	22	6	2	26g
23	1%Pd50@Au50/TiO_2 calc. 673K	none	393	10	1/55000	8650	72	21	5	2	26g
24	1%Au50@Pd50/TiO_2 calc. 673K	none	393	10	1/55000	8780	69	25	4	1	26g
25	1%Au50+Pd50/AC calc. 673K	none	393	10	1/55000	2490	79	2	10	4	26g
26	1%Pd50@Au50/AC calc. 673K	none	393	10	1/55000	2430	75	3	13	4	26g
27	1%Au50@Pd50/AC calc. 673K	none	393	10	1/55000	3410	79	5	11	4	26g
28	1%Pd40@(Au60/CNFs)	none	393	1.5	1/35000	6076	74	18	3	1	64
29	1%Pd40@(Au60/N-CNFs)	none	393	1.5	1/35000	52638	76	11	7	5	64
30	2%Au70+Pd10/PANI[a]	toluene	373	1	1/150	16	71	nd	nd	nd	21
31	2%Au50+Pd50/PANI[a]	toluene	373	1	1/150	16	82	nd	nd	nd	21
32	2%Au10+Pd90/PANI[a]	toluene	373	1	1/150	14	98	nd	nd	nd	21
33	3Au-1Pd/APS-S16	none	413	1	nd	4052	89	11	nd	0	65
34	1Au-1Pd/APS-S16	none	413	1	nd	4715	94	6	nd	0	65
35	1Au-2Pd/APS-S16	none	413	1	nd	6575	94	5	nd	1	65
36	1Au-3Pd/APS-S16	none	413	1	nd	7864	91	8	nd	1	65
37	1Au-5Pd/APS-S16	none	413	1	nd	8667	94	5	nd	1	65
38	1%Au-0.5%Pd/γ-Al_2O_3	toluene	333	1	1/500	5.5	81	-	19	-	63
39	1%Au+0.5%Pd/γ-Al_2O_3	toluene	333	1	1/500	26.4	84	-	14	-	63
40	1%Pd40@(Au60/AC)	cyclohexane	353	2	1/5000	2261	89	8	2	1	68
41	0.1%Bi+1%Pd40@(Au60/AC)	cyclohexane	353	2	1/5000	2546	95	2	3	0	68
42	3%Bi+1%Pd40@(Au60/AC)	cyclohexane	353	2	1/5000	1643	97	1	2	0	68
43	1%Au50+Pd50/TiO_2	none	393	10	1/100000	63800	67	3	7	23	69
44	1%Au45+Pd45+Pt10/TiO_2	none	393	10	1/100000	31900	80	-	6	13	69

a)Addition of NaOH

amount with all the catalysts (entry 7-10, table 1). Another interesting study from this group showed that AuPd alloy was in situ formed starting from a physical mixture of Au/AC and Pd/AC in the benzyl alcohol oxidation in water. After 1h of reaction the physical mixture showed a similar catalytic activity than AuPd/AC alloy. TEM characterization performed on the used catalyst, showed the partial formation of AuPd alloy, probably due to the migration of Pd species onto Au nanoparticles.[58]

Hutchings' group extensively studied the effect of AuPd morphology, in particular when supported on TiO_2, in alcohols oxidation. They showed that AuPd alloys, prepared by impregnation method, are particularly efficient for the solvent free benzyl alcohol oxidation in presence of molecular oxygen.[11b] Under these reaction conditions, very high activities were detected, with TOFs values that increased from 14270 h^{-1} to 86500 h^{-1}, increasing the reaction temperature from 383K to 433K (entry 11-13, table 1). The high activity was attributed to the formation of Au-rich core/ Pd-shell structure, with an electron promotion effect for Au on Pd.[11b] Also for these systems the effect of Au:Pd ratio has been investigated and it was determined that AuPd 1:1 weight ratio produced the highest catalytic activity.[31b] Interestingly it was reported that Au/Pd ratio has an important effect also on the selectivity. Indeed, with Pd-rich composition a selectivity of 66-70% to benzaldehyde was observed with the production of 21% of toluene, whereas Au-rich composition yield to 95% of benzaldehyde, depressing the formation of tol, uene. In following studies the same group compared the catalytic activity of AuPd catalysts supported on activated carbon prepared by sol immobilization (entry 14, table 1) and by impregnation (entry 15, table 1). In both cases an homogenous alloy was obtained. The higher catalytic performance of AuPd prepared by sol immobilization was attributed to the different particle size, and size distribution. Indeed, it is well accepted, that liquid phase oxidation is a size-dependent reaction, where smaller particles are more active than bigger ones.[7] Indeed, for sol immobilization prepared ones, AuPd particles of 5nm have been obtained, whereas for the ones prepared by impregnation larger AuPd particles of 3-8 nm, with the presence of different particles >20 nm.[59] The effect of random alloy versus core-shell structure has been also investigated, preparing AuPd nanoparticles via sol immobilization and using titania and activated carbon as supports.[27g,28] For this purpose, AuPd nanoparticles were synthesize by co-reduction of the two metals (Au+Pd) or by sequential reduction of Au and Pd (Pd@Au) or vice versa (Au@Pd). STEM-HAADF confirmed that AuPd alloy was obtained by co-reduction, whereas core-structure was created by sequential addition of the two metals. The catalyst were tested in the benzyl alcohol oxidation in solventless condition at 393K (entry 16-27, table 1). The order of metal addition has a significant effect on the catalytic activity, and the most active catalyst resulted Aucore-Pdshell, regardless the support used (entry 17 and 20, table 1). On the contrary the order of metal addition did not appreciably influence the selectivity.

The support has a stronger effect on both activity and the selectivity addition: AC supported ones showed a better activity (entry 19-21,table 1), whereas TiO_2 supported ones showed a better selectivity to benzaldehyde with a limited production of toluene (entry 16-18,table 1).

In these studies, calcination treatment has been performed (673K in air) in order to remove the PVA from the metal surface and to investigate the effect of PVA on the catalytic performance has been investigated.[27g,28] The high temperature used efficiently removed the PVA form the surface, but affecting the morphology of the catalyst, with a general growing of the AuPd particles, more evident in the activated carbon supported ones.[28] As a consequence, all the catalysts resulted less active than untreated one (entry 23-27, table 1).

Beyond PVA, other protective agents have been proposed for the generation of AuPd nanoparticles, to be used in this reaction. Baiker's group, for example, reported the synthesis of THPC protected AuPd nanoparticles supported on PANI varying the AuPd ratio from 7-1 to 1-9 and the utilization in the oxidation of benzyl alcohol, using water as solvent and NaOH.[22] The catalysts reached full conversion but they did not show an appreciable TOF (14-16 h^{-1}) compared to the previously reported systems even in presence of NaOH (entry 30-32, table 1). It is also interesting to note that a very high selectivity to benzaldehyde has been achieved, (71-98%) compared to AuXPdY/AC previously described (28-50%) (entry 7-10, table 1). Benzoic acid was not detected, and they probably addressed the absence the formation of amides formed from benzoic acid and the amines present on PANI.[22]

Different groups developed different strategies, such as incipient wetness,[60] grafting,[61] and Ar glow-discharge plasma reduction,[62] for introducing the AuPd nanoparticles inside the framework of SBA-15 to increase the stability of the catalytic systems during the reaction. The catalysts showed a good resistance to deactivation during recycling tests, due to limited leaching of the metal, probably due to a steric confinement inside the mesopores of SBA-15.

Evangelisti et al. proposed an alternative procedure to generate supported AuPd nanoparticles by metal vapor synthesis using alumina as support. They showed that the AuPd alloy system prepared by direct vaporization of the two metals (entry 39, table 1) is more active than the physical mixing of separate prepared Au and Pd precursors (entry 38 ,table 1), as already point out for wet preparation synthesis.[63]

Recently it has been shown that the support is an important factor determining the overall activity of metal nanoparticles in particular in the liquid phase reaction.[5a,b] Indeed, the support properties can create different interactions with the metallic particles immobilized on the surface or inside the pore structure, thus modifying both their electronic and structural properties. In addition the support can also provide different anchoring sites for the reactant, or play an active role in the catalytic reaction. It is normally recognized that surface acid and basic functionalities provide a better dispersion of MNPs which contributes to an increase of the catalytic activity. On the

other hand, basic functionalized surface can speed up the oxidation rate, favoring the H-abstraction.

Many studies are present in the literature dedicated the support effect for Au or Pd nanoparticles. However only few examples are present for bimetallic AuPd.

Villa et al. reported the immobilization of PVA protected AuPd nanoparticles on bare (CNFs) and nitrogen functionalized carbon nanofibers (N-CNFs).[64] Nitrogen groups were introduced in the support framework by gas phase treatment with ammonia at 873, increasing the basicity of the support. The improvement in the catalytic performance of AuPd/N-CNFs, in the solvent free benzyl alcohol oxidation, was attributed to a better dispersion of the metal nanoparticles on the surface, as well as to the increased local basic environment, compared to AuPd/CNFs (entry 28, 29, table 1).

A similar strategies was adopted by Chen et al., impregnating AuxPdy onto amino functionalized SBA-16. All the catalysts, consisting in pure alloy revealed a good activity in the solventless oxidation of benzyl alcohol, being the Pd-rich composition the most active (entry 33-37, table 1). Moreover, the presence of amino groups increases the durability of the catalyst maintaining the same catalytic performance during recycling tests.[65]

AuPd nanoalloys supported on Mg-Al oxides showed a better performance than CeO_2 and SiO_2 supported ones, due, according to the authors, to the strong dehydrogenation ability of Mg-Al oxide, facilitating the H-abstraction.[66]

In all the studies reported it has been shown that the main problematic that affect the selectivity to benzaldehyde during benzyl alcohol oxidation is the parallel production of toluene. Two principal mechanisms were proposed for toluene formation, the disproportionation of two molecules of benzyl alcohol to form equimolar benzaldehyde and toluene or by reaction of the intermediate metal-hydride with alcohol instead of O_2.[6]

Recent literature reported different strategies in order to depress the toluene formation, in particular the design of new catalysts, varying the support or introducing a metal that acts as modifier of the AuPd active sites. Sankar et al. showed that in the case of $AuPd/TiO_2$ the disproportionation of benzyl alcohol is the main source of toluene.[67] By choosing the appropriate supports, such as MgO and ZnO, the disproportionation reaction is depressed, with consequent increase of benzaldehyde.[67] Prati's group showed that the addition of 0.1%Bi and 3%Bi to AuPd/AC increased the selectivity to benzaldehyde from 89% for AuPd to 95-97% for 0.1%Bi-AuPd and 3%Bi-AuPd, respectively.[68] This effect could be mainly ascribed to the blocking of a fraction of active sites, responsible of a different substrate coordination. In this case the parallel pathway that yield to toluene has been suppressed. However the amount of Bi introduced in AuPd has a different effect on the activity. The addition of 0.1% Bi has a positive effect on the activity of the catalyst (TOF: 2546 h^{-1} and 2261 h^{-1} for 0.1%Bi-AuPd and AuPd, respectively) (entry 40-41,table 1). On the contrary for higher loading (3%) Bi has a detrimental effect (TOF: 1643 h^{-1}) (entry 42, table 1). The promotional effect of Bi can be attributed to an electronic effect. However when Bi is present in higher amount it can block some AuPd active sites.

Similarly, He et al., showed that the addition of Pt to $AuPd/TiO_2$, with the formation of random ternary alloy, decreases the activity but increases the selectivity to benzaldehyde from 67% to 80% depressing the formation of toluene and limiting the formation of benzoic acid (entry 43, 44, table 1).[69]

CO oxidation

Catalytic oxidation of CO has been extensively studies, in particular using monometallic catalyst. On the contrary, only few examples on the use of Au bimetallic catalysts in particular AuPd, are present.[15a] The reaction can be presented by the equation: $CO + 0.5O_2 \rightarrow CO_2$ and can be considered the pivotal reaction which mostly contribute to the success of gold in catalysis.

The first attempt of using AuPd bimetallic catalyst involved the use of catalysts prepared by sol immobilization of protected AuPd nanoparticles. It should be highlighted however that the protective agent has to be removed from the metal surface, for example by heat treatment, in order to obtain active catalysts for the gas phase CO oxidation. Conversely, this post-treatment is not required for the liquid phase oxidation where the protective agent only partially decrease the catalytic performance. The reason of the different trend is still not clear. Probably in the liquid phase the solvent is able to remove the protective agent from the active site during the reaction. On the other hand, the protective layer branches can have a different geometrical structure in the two phases, making the active site accessible to the reactant only in the liquid phase.

Guczi's group was the first to report the synthesis of AuPd bimetallic system for this reaction. AuPd nanoparticles were generated in presence of tannin and citrate, that act as protective and reducing agent, and then supported on TiO_2.[24] The samples were calcined at 400°C for 1h in a O_2/He mixture in order to remove the protective agents from metal surface and then reduced in H_2 at 200°C. This treatment was efficient in the removal of the organic layer but yielded to particles growth from 4.3 to 9.6 nm. XAS characterization evidenced the presence of AuPd alloy, even segregated Pd was not excluded. Surprisingly, CO oxidation, performed at 60°C with a mixture of 5.6 mbar CO and 91.8 mbar O_2 in He, showed that the activity of AuPd bimetallic system is only slightly higher than the activity of Au-Pd physical mixture, evidencing only a minimal synergistic effect. The authors in a successive study, compared $AuPd/TiO_2$ prepared by using the same methodology investigating the effect of co-reduction or sequential reduction of the two metals.[70] An alloy structure has been found in all the cases and XPS revealed a Pd enrichment in the case of Pd deposited on Au. The three different bimetallic systems obtained showed however a similar activity. Therefore the activity seems not to be significantly influenced by the surface composition of the bimetallic systems. Moreover, it has been

observed that, like in previous report, the AuPd alloy is almost as active as the Au+Pd physical mixture.

The same group reported the synthesis of AuPd nanoparticles supported on silica, prepared via sol immobilization using PVP as stabilizer.[25] The stabilizer has been removed through calcination at 673K before testing the catalyst in CO oxidation at 413K. The effect of Au/Pd ratio has been studied and it has been varied from 1-9 to 9-1 (molar ratio). XRD measurement evidenced the presence of AuPd alloy, with mean particle size of 12-24 nm after calcination. All the catalysts did not show a high activity compared to data present in the literature, probably sue to the large size of AuPd nanoparticles. In these two cases the limited synergistic effect is due to the absence of an homogenous alloy but to the presence of both alloyed and segregated metals.

Scott et al. reported the synthesis of AuPd catalysts prepared using amino-terminated poly(amidoamine) dendrimer-encapsulated nanoparticles, using $NaBH_4$ as reducing agent.[71] AuPd nanoparticles were supported on TiO_2, and calcined at 773K in O_2 to remove the organic layer from the metal surface, and then treated in H_2 flow. The AuPd average particles size only slightly increased during the calcination step, from 1.8 to 3.2 nm. EDS analyses of individual nanoparticles confirmed the presence of AuPd alloy with almost the same atomic composition. Interestingly in this case a strong synergistic effect has been evidenced. Indeed AuPd starts to be active a 150°C, where Au and Pd monometallic ones are completely inactive.

El-Shall et al. proposed a microwave irradiation method for the preparation of AuPd nanoparticles in a mixture of oleyl amine and oleic acid as capping and reducing agent and supported on CeO_2.[72] The presence of AuPd alloy was proved through XRD and TEM measurements. AuPd alloy showed a higher activity compared to monometallic Pd only at low temperature (<333K).

TiO_2-supported AuPd with Au/Pd atomic ratio of 8 was prepared by deposition-precipitation with urea, followed by reduction under H_2 at 773K.[73] XPS and diffuse reflectance infrared Fourier transform spectroscopy (DRIFTs) analysis evidenced the presence of AuPd alloy with partial segregation of Au. Interestingly, AuPd surface composition was monitored by environmental high resolution electron microscopy (ETEM) and (DRIFTs) during the exposure to O_2 and CO/O_2, evidencing Pd segregation at the surface with the formation of Au_{core}-Pd_{shell} structure. AuPd alloy showed a better activity in the low temperature CO oxidation than monometallic Au. However, the Authors observed a higher rate of deactivation in $AuPd/TiO_2$ compared to Au/TiO_2, probably due to the replacement of Au in low coordination sites, that are considered the most active site in CO oxidation, by Pd atoms.[74]

Goodman and co-workers investigate CO oxidation on planar AuPd surfaces deposited on Mo(110) as well as on TiO_2 supported AuPd nanoparticles to understand the synergistic effect of AuPd alloy compared to monometallic Pd and Au, using Polarization-Modulation Infrared Reflection Absorption Spectroscopy (PM-IRAS) and kinetic studies.[75] At low pressure ($1.3*10^{-7}$ mbar) Pd resulted more active than corresponding AuPd alloy. Indeed, alloying Au with Pd isolated Pd sites are formed which are not able to dissociate O_2.[76] It should be noted indeed, that chemisorbed O_2 must react as dissociate oxygen in order to form CO_2. At higher pressure (20 mbar), reaction conditions at which are normally performed the studies cited above, Pd preferentially segregated at the surface, as evidenced by Delannoy et, form contiguous Pd sites, able to dissociate O_2.[77]

Moreover, Pd deactivates faster than AuPd, due to the stronger CO binding and tendency to be passivate by oxygen than the alloy surface.

Concluding remarks

Gold has been studied for a long time as a potential alternative to Pd or Pt catalysts. Indeed its catalytic activity has been shown to be often advantageous especially in terms of selectivity and durability. Therefore a lot of efforts have been done to combine the peculiar properties of gold with the already well-established ones of other catalytically active metals.

Taking the case of Pd based catalysts, this paper reviewed the main results obtained with the addition of Au for two specific applications, namely the oxidation of benzylic alcohol in the liquid phase and CO oxidation in the gas phase. It clearly appears that the effect of modifying the Pd catalysts with Au can have different sorts depending of the nature of the bimetallic species, even if generally a positive effect has been claimed.

Particular attention should be paid to the real nature of the obtained bimetallic specie as it strongly affects catalytic activity and selectivity. Therefore the characterization of the representative species plays a crucial role in determining the catalytic properties. Moreover, it has been shown that this task is not trivial and should be carefully checked to be really representative to the whole catalytic material.

Notes and references

[a] Dipartimento di Chimica, Università degli Studi di Milano, via Golgi 19, 20133Milano, Italy.
email:Laura.Prati@unimi.it

[b] Institut für Nanotechnologie, Karlsruher Institut für Technologie, Hermann-von-Helmholtz-Platz 1, 76344 Eggenstein-Leopoldshafen, Germany.

[c] Department of Inorganic Chemistry, Fritz Haber Institut of the Max Planck Society, Faradayweg 4-6, Berlin 14195, Germany.

[d] Shenyang National Laboratory for Materials Science Institute of Metal Research Chinese Academy of Sciences 72 Wenhua Road, Shenyang 110016 (China)

1 a) M. A. El-Sayed, *Acc. Chem. Res.,* 2001, **34**, 257; b) K.G. Thomas, A.V. Kamat, *Acc. Chem. Res*., 2003, **36**, 888; c) M. C. Daniel and D. Astruc, *Chem. Rev.*, 2004, **104**, 293; E.C.

Dreaden, A. M. Alkilany, X. Huang, C. J. Murphy and M. A. El-Sayed, *Chem. Soc. Rev.*, 2012, **41**, 2740; Y. Zhang, X. Cui, F. Shi, and Y. Deng, *Chem. Rev.,* 2012, **112**, 2467.

2 M. Haruta, T. Kobayashi, H. Sano, N. Yamada, *Chem. Lett*. 1987, 405.

3 G.J. Hutchings, *J. Catal.*, 1985, **96**, 292.

4 a) G.C. Bond, D.T. Thompson, *Catal. Rev. Sci. Eng.*, 1999, **41**, 319; b) G.C. Bond, C. Louis, D. T. Thompson, ed. G. J. Hutchings, ICP Covent Garden, London, 2006, Catalytic Science Series, vol. 6.

5 a) M. Haruta, *Catal Today*, 1997, **36** (1), 153; b) L. Prati, A. Villa, A. R. Lupini and G. M. Veith, *Phys. Chem. Chem. Phys.*, 2012, **14**, 2969; c) A. Villa, M. Schiavoni and L. Prati, *Catal. Sci. Technol.*, 2012, **2**, 673; d) X. Y. Liu, A. Wang, T. Zhang, C-Y. Mou, *Nano Today*, 2013, **8**, 403.

6 T. Mallat, A. Baiker, *Chem. Rev.*, 2004, **104**, 3037.

7 a) S. Carrettin, P. McMorn, P. Johnston, K. Griffin, C. J. Kiely, G. J.Hutchings, *Phys. Chem. Chem. Phys*., 2003, **5**, 1329 ; b) F. Porta, L. Prati, *J. Catal*., 2004, **224**, 397.

8 A. K. Singh, Q. Xu, *Chem. Cat. Chem*., 2013, **5**, 652.

9 a) N. Dimitratos, J. A. Lopez-Sanchez, G. J. Hutchings, *Chem. Sci.,* 2012, **3**, 20; b) S. E. Davis, M. S. Ide, R. J. Davis, *Green. Chem.*, 2013, **15**, 17.

10 a) C. George, A. Genovese, A. Casu, M. Prato, M. Povia, L. Manna and T. Montanari, *Nano Lett.*, 2013, **13**, 752; b) J. Xu, T. White, P. Li, C. He, J. Yu, W. Yuan and Y.-F. Han, *J. Am. Chem. Soc.*, 2010, **132**, 10398.

11 a) N. Dimitratos, A. Villa, D. Wang, F. Porta, D. Su, Laura Prati, *J. Catal.*, 2006, **244**, 113; b) D. I. Enache, J. K. Edwards, P. Landon, B. Solsona-Espriu, A. F. Carley, A. A. Herzing, M. Watanabe, C. J. Kiely, D. W. Knight and G. J. Hutchings, *Science*, 2006, **311**, 362.

12 J. K. Edwards, S. J. Freakley, A. F. Carley, C. J. Kiely, and G. J. Hutchings, *Acc. Chem. Res*, 2014, **47**, 845.

13 L. Kesavan, R. Tiruvalam, M. H. A. Rahim, M. I. bin Saiman,D. I. Enache, R. L. Jenkins, N. Dimitratos, J. A. Lopez- Sanchez, S. H. Taylor, D. W. Knight, C. J. Kiely and G. J. Hutchings, *Science*, 2011, **331**, 195.

14 a) D. Martin Alonso, S. G. Wettsteina and J. A. Dumesic, *Chem. Soc. Rev.*, 2012, **41**, 8075; b) H. Zhanga and N. Toshima, *Catal. Sci. Technol.*, 2013, **3**, 268.

15 a) A. Kumar Singh and Q. Xu, *Chem. Cat. Chem*., 2013, **5**, 652; b) A. Wanga, X. Y. Liu, C.-Y. Moub, T. Zhang, *J. Catal.*, 2013, **308**, 258.

16 R. Ferrando, J. Jellinek, R. L. Johnston, *Chem. Rev.*, 2008, **108**, 845.

17 a) M. A. K. Khalil, R. A. Rasmussen, *Science*, 1984, **224**, 54; b) X. W. Xie, Y. Li, Z. Q. Liu, M. Haruta, W. J. Shen, *Nature* 2009, **458**, 746.

18 a) M. V. Twigg, *Appl. Catal. B*, 2007, **70**, 2; b) R. M. Heck, R. J. Farrauto, *Appl. Catal. A*, 2001, **221**, 443; c) S. Royer, D. Duprez, *Chem. Cat. Chem*., 2011, **3**, 24.

19 Q. Fu, W. X. Li, Y. X. Yao, H. Y. Liu, H. Y. Su, D. Ma, X. K. Gu, L. M. Chen, Z. Wang, H. Zhang, B. Wang, X. H. Bao, *Science*, 2010, **328**, 1141.

20 a) H. Boennemann and R. M. Richards, *Eur. J. Inorg. Chem*., 2001, 2455; b) C. Burda, X. Chen, R. Narayanan and M. A. El-Sayed, *Chem. Rev.*, 2005, **105**, 1025; c) C. N. R. Rao, G. U. Kulkarni, P. J. Thomas and P. P. Edwards, *Chem. Soc. Rev*., 2000, **29**, 27.

21 V. K. Lamer, R. H. Dinegar, *J. Am. Chem. Soc*., 1950, **72**, 4847.

22 S. Marx and A. Baiker, *J. Phys. Chem. C*, 2009, **113**, 6191.

23 D. A. Handley, In Colloidal Gold: Principles, Methods and Applications (Ed.: M. A. Hayat), Academic, San Diego, CA, 1989.

24 L. Guczi, A. Beck, A. Horváth, Zs. Koppány, G. Stefler, K. Frey, I. Sajó, O. Geszti, D. Bazin, J. Lynch, *J. Mol. Catal. A: Chemical*, 2003, **204–205**, 545.

25 A. M. Venezia, L. F. Liotta, G. Pantaleo, V. La Parola, G. Deganello, A. Beck, Zs. Koppány, K. Frey, D. Horváth, L. Guczi, *Appl. Catal. A: General*, 2003, **251**, 359.

26 M. Sankar, N. Dimitratos, P. J. Miedziak, P. P. Wells, C. J. Kielye and G. J. Hutchings, *Chem. Soc. Rev*., 2012, **41**, 8099.

27 a) N. Dimitratos, F. Porta, L. Prati, *Appl. Catal. A:General*, 2005, **291**, 210; b) C. L. Bianchi, P. Canton, N. Dimitratos, F. Porta, L. Prati, *Catal. Today*, 2005, **102-103**, 203; c) M. Comotti, C. Della Pina, M. Rossi, J. *Mol. Catal. A: Chemical*, 2006, *251*, 89-; d) N. Dimitratos, C. Messi, F. Porta, L. Prati, A. Villa, *J. Mol. Catal. A: General*, 2006, **256**, 21; e) N. K. Chaki, H. Tsunoyama, Y. Negishi, H. Sakurai, T. Tsukuda, *J. Phys. Chem. C*, 2007, **111**, 4885; f) J.A. Lopez-Sanchez, N. Dimitratos, P. Miedziak, E. Ntainjua, J. E. Edwards, D. Morgan, A. F. Carley, R. Tiruvalam, C. J. Kiely, G. J. Hutchings, *Phys. Chem. Chem. Phys.* 2008, **10**, 1921; g) N. Dimitratos, J. A. Lopez- Sanchez, D. Morgan, A. F. Carley, R. Tiruvalam, C. J. Kiely, D. Bethell, G. J. Hutchings, *Phys. Chem. Chem. Phys*., 2009, **11**, 5142; h) J. Pritchard, L. Kesavan, M. Piccinini, Q.He, R. Tiruvalam, N. Dimitratos, J. A. Lopez-Sanchez, A. F. Carley, J. K. Edwards, C. J. Kiely, G. J. Hutchings, *Langmuir*, 2010, **26**, 16568.

28 R. C. Tiruvalam, J. C. Pritchard, N. Dimitratos, J. A. Lopez-Sanchez, J. K. Edwards, A.F. Carley, G. J. Hutchings, C. J. Kiley, *Faraday Discuss*. 2011, **152**, 63.

29 D. Wang, A. Villa, F. Porta, D. Su, L. Prati, *Chem. Comm.*, 2006, 1956.

30 a) A. Villa, C. Campione, and L. Prati, *Catal. Lett.*, 2007, **115**,133; b) D. Wang, A. Villa, F. Porta, L. Prati, and D. Su, J. *Phys. Chem. C,* 2008, **112**, 8617.

31 A. Villa, D. Wang, D. Su, G. M. Veith and L. Prati, *Phys. Chem. Chem. Phys.*, 2010, **12**, 2183.

32 a) G. Li, D. I. Enache, J. Edwards, A. F. Carley, D. W. Knight, G. J. Hutchings, *Catal. Lett.*, 2006, **110**, 7; b) D. I. Enache, D. Barker, J. K. Edwards, S.H. Taylor, D. W. Knight, A. F. Carley, G. J. Hutchings, *Catal Today 2007*, **122**, 407; c) P. J. Miedziak, Z. Tang, T. E. Davies, D. I. Enache, J. K. Bartley, A. F. Carley, A. A. Herzig, C. J. Kiely, S. H. Taylor, G. J. Hutchings, *J. Mater. Chem.* 2009, **19**, 8619.

33 G. J. Hutchings, and C. J. Kiely, Acc. Chem. Res, 2013, 46, 1759.

34 A. Denton and N. Ashcroft, *Phys. Rev. A*, 1991, **43**, 3161–3164.
35 H. M. Rietveld, *J. Appl. Crystallogr.*, 1969, **2**, 65–71.
36 A. Patterson, *Phys. Rev.*, 1939, **56**, 978–982.
37 B. W. Reed, D. G. Morgan, N. L. Okamoto, A. Kulkarni, B. C. Gates, and N. D. Browning, *Ultramicroscopy*, 2009, **110**, 48–60.
38 A. Carlsson, A. Puig-Molina, and T. V. W. Janssens, *J. Phys. Chem. B*, 2006, **110**, 5286–5293.
39 S. Hüfner, Photoelectron Spectroscopy - Principles and Applications, 2003, Springer,
40 A. A. Herzing, M. Watanabe, J. K. Edwards, M. Conte, Z.-R. Tang, G. J. Hutchings, and C. J. Kiely, *Faraday Discuss.*, 2008, **138**, 337–351.
41 F. Liu, D. Wechsler, and P. Zhang, *Chem. Phys. Lett.*, 2008, **461**, 254–259.
42 S. Nishimura, Y. Yakita, M. Katayama, K. Higashimine, and K. Ebitani, *Catal. Sci. Technol.*, 2013, **3**, 351.
43 Y. Shi, H. Yang, X. Zhao, T. Cao, J. Chen, W. Zhu, Y. Yu, and Z. Hou, *Catal. Commun.*, 2012, **18**, 142–146.
44 D. C. Koningsberger, R. Prins (eds.), X-ray Absorption: Principles, Applications, Techniques of EXAFS, SEXAFS, and XANES, 1987, Wiley.
45 W. Ketchie, M. Murayama, and R. Davis, *J. Catal.*, 2007, **250**, 264–273.
46 N. Tanaka, *Sci. Technol. Adv. Mater.*, 2008, **9**, 014111.
47 S. J. Pennycook and D. E. Jesson, *Ultramicroscopy*, 1991, **37**, 14–38.
48 M. Tsuji, K. Ikedo, M. Matsunaga, and K. Uto, *CrystEngComm*, 2012, **14**, 3411.
49 P. Dash, T. Bond, C. Fowler, W. Hou, N. Coombs, and R. W. J. Scott, *J. Phys. Chem. C*, 2009, **113**, 12719–12730.
50 M. Heggen, M. Oezaslan, L. Houben, and P. Strasser, *J. Phys. Chem. C*, 2012, **116**, 19073–19083.
51 G. J. Hutchings, *Chem. Commun. (Camb).*, 2008, 1148–64.
52 H. Zhang and N. Toshima, *Catal. Sci. Technol.*, 2013, **3**, 268.
53 Q. He, P. J. Miedziak, L. Kesavan, N. Dimitratos, M. Sankar, J. A. Lopez-Sanchez, M. M. Forde, J. K. Edwards, D. W. Knight, S. H. Taylor, C. J. Kiely, and G. J. Hutchings, *Faraday Discuss.*, 2013, **162**, 365.
54 D. Ferrer, A. Torres-Castro, X. Gao, S. Sepúlveda-Guzmán, U. Ortiz-Méndez, and M. José-Yacamán, *Nano Lett.*, 2007, **7**, 1701–5.
55 D. Wang, A. Villa, P. Spontoni, D. S. Su, and L. Prati, *Chemistry a European Journal*, 2010, **16**, 10007–13.
56 A. Villa, D. Wang, N. Dimitratos, D. Su, V. Trevisan, L. Prati, *Catal. Today*, 2010, **150**, 8.
57 A. Villa, N. Janjic, P. Spontoni, D. Wang, D. S. Su, L. Prati, *Appl. Catal. A: General*, 2009, **364** 221.
58 D. Wang, A. Villa, P. Spontoni, D. S. Su, and L. Prati, *Chem. Eur. J.*, 2010, **16**, 10007.
59 J. A. Lopez-Sanchez, N. Dimitratos, N. Glanville, L. Kesavan, C. Hammond, J. K. Edwards, A. F. Carley, C. J. Kiely, G. J. Hutchings, *Appl. Catal. A: General*, 2011, **391**, 400.
60 Y. Hao, G.-P. Hao, D.-C. Guo, C.-Z. Guo, W.-C. Li, M.-R. Li, and A.-H. Lu, *Chem. Cat. Chem.*, 2012, **4**, 1595.
61 C. Y. Ma, B. J. Dou, J. J. Li, J. Cheng, Q. Hu, Z. P. Hao, S. Z. Qiao, *Appl. Catal. B: Environmental*, 2009, **92**, 202.
62 Y. Chen, H. Wang, C.-J. Liu, Z. Zeng, H. Zhang, C. Zhou, X. Jia, Y. Yang, *J. Catal.*, 2012, **289**, 105.
63 C. Evangelisti, E. Schiavi, L. A. Aronica, A. M. Caporusso, G. Vitulli, L. Bertinetti, G. Martra, A. Balerna, S. Mobilio, J. *Catal.*, 2012, **286**, 224.
64 A.Villa, D. Wang, P. Spontoni, R. Arrigo, D. Su, L. Prati, *Catal. Today*, 2010, **157**, 89.
65 Y. Chen, H. Lim, Q. Tang, Y. Gao, T. Sun, Q. Yan, Y. Yang, Appl. Catal. A: General, 2010, 380, 55.
66 L. Wang, W. Zhang, S. Zeng, D. Su, X. Meng, F. Xiao, *Chin. J. Chem.*, 2012, **30**, 2189.
67 M. Sankar, E. Nowicka, R. Tiruvalam, Q. He, S. H. Taylor, C. J. Kiely, D. Bethell, D. W. Knight, and G. J. Hutchings, Chem. Eur. J., 2011, 17, 6524.
68 A. Villa, D. Wang, G. M. Veith, L. Prati, *J. Catal.*, 2012, **292**, 73.
69 Q. He, P. J. Miedziak, L. Kesavan, N. Dimitratos, M. Sankar, J. A. Lopez-Sanchez, M. M. Forde, J. K. Edwards, D. W. Knight, S. H. Taylor, C. J. Kiely and G. J. Hutchings, *Faraday Discuss.*, 2013, **162**, 365.
70 A. Beck, A. Horvath, Z. Schay, Gy. Stefler, Zs. Koppany, I. Sajo´, O. Geszti, and L. Guczi, *Top. Catal.*, 2007, **44**, 115.
71 R. W. J. Scott, C. Sivadinarayana, O. M. Wilson, Z. Yan, D. W. Goodman, and R. M. Crooks, *J. Am. Chem. Soc*. 2005, **127**, 1380.
72 V. Abdelsayed, A. Aljarash, and M. S. El-Shall, *Chem. Mater*. 2009, **21**, 2825.
73 L. Delannoy, S. Giorgio, J. G. Mattei, C. R. Henry, N. El Kolli, C. Methivier, and C. Louis, *Chem. Cat. Chem*., 2013, **5**, 2707.
74 M. Haruta, S. tsubota, T. Kobayashi, H. Kageyama, M. J. Genet, B. Delmon, *J. Catal.*, 1993, **144**, 175.
75 F. Gao, Y. Wang, D. W. Goodman, *J. Phys. Chem. C*, 2010, **114 (9)**, 4036.
76 Z. Li, G. GaO, W. T. Tysoe, *J. Phys. Chem. C*, 2010, **114**, 16909.
77 Z. Li, G. GaO, W. T. Tysoe, *J. Phys. Chem. C*, 2010, **114**, 16909.